The Role of Diameter Variation in Investigation of Coronary Tortuosity

Author:
Shen, Chi; Zhang, Mingzi; Beier, Susann

Publication details:
Proceedings of the 23rd Australasian Fluid Mechanics Conference
pp. 1 - 6
2653-0597 (ISSN)

Event details:
The 23rd Australasian Fluid Mechanics Conference – 23AFMC
Sydney
2022-12-04 - 2022-12-08

Publication Date:
2022-12-08

DOI:
https://doi.org/10.26190/unsworks/28731

23rd Australasian Fluid Mechanics Conference – 23AFMC
Sydney, Australia
4-8 December 2022
Paper No: AFMC2022-241

The Effect of Diameter Variation when accessing Patient-specific Coronary Tortuosity

C. Shen [1*], M. Zhang [1] and S. Beier [1]

[1] School of Mechanical and Manufacturing Engineering, Faculty of Engineering,
University of New South Wales, Sydney NSW 2052, Australia

* Email: chi.shen@student.unsw.edu.au

Abstract

Coronary diameter and tortuosity are two important morphological parameters that both affect the local haemodynamics. However, previous studies on tortuous coronaries neglected any potential associated effects from vascular diameter variations. Here, we investigate the differences in coronary haemodynamics due to diameter variation in tortuous coronaries. 28 models were derived from modifications of four non-bifurcating and bifurcating coronaries each. For the non-bifurcating coronaries, we first generated a uniform cross-sectional diameter model, before scaling it by + and -1 mm. For the bifurcations, we only scaled the models by + and -1 mm. The computational results showed that the vascular diameter had a great effect on the haemodynamics of torturous arteries. For non-bifurcating models, the modified geometries with constant diameters exhibited a small change in the local velocity field and a smaller percentage vessel area exposed to adverse time-average wall shear stress (TAWSS%), compared to their original coronaries with varying diameters. Moreover, the TAWSS% increased in the modified geometries with constant diameters as the diameter increased. For the bifurcating models with varying diameters, both helicity intensity (h_2) and TAWSS% were 24%, 33% less in -1 mm-smaller models, and 31%, 44% larger in +1 mm-larger models, compared to the original equivalents. Overall, the effect of tortuosity on haemodynamics, commonly measured as centreline index, cannot be considered independently of the vessel diameter and potentially other shape characteristics. This may explain contradicting findings in previous literature to date and thus warrants future studies.

1. Introduction

Coronary artery tortuosity is a phenomenon commonly observed in vivo, which affects the local blood flow patterns and haemodynamics of clinical relevance (Kahe et al. 2020). However, the effect of coronary tortuosity remains inconclusive, with contradicting findings from both in vivo and computational studies. Specifically, some in vivo studies reported that coronary tortuosity is associated with plaque formation (El Tahlawi et al. 2016; Kahe et al. 2020), whereas others have shown a protective effect against plaque formation (Li et al. 2018; Khosravani-Rudpishi, Joharimoghadam, and Rayzan 2018). Likewise, some computational studies revealed that adverse haemodynamics are prominent in severely tortuous regions (Xie et al. 2014; Buradi and Mahalingam 2020; Xie, Wang, and Zhou 2013), whereas others claimed that tortuosity can reduce the area exposed to adverse time-averaged wall shear stress (TAWSS) (Rabbi, Laboni, and Arafat 2020; Vorobtsova et al. 2016).

Tortuosity as a measure has not been commonly defined until recently, and in a recent study, the absolute curvature was recommended as a benchmark measure (Kashyap et al. 2022). Regardless of the measurement method used, tortuosity is simply a centreline index that does not take into account any concomitant variations in other shape parameters, such as the changing cross-sectional vascular diameter — an important coronary morphological parameter especially for tortuous arterial segments (Muller et al. 2012). Previous studies on tortuosity have either used idealised models with

constant diameters (Xie et al. 2014; Buradi and Mahalingam 2020; Xie, Wang, and Zhou 2013; Rabbi, Laboni, and Arafat 2020), or assessed haemodynamic changes with respect to tortuosity only, without considering the concomitant effects of diameter (Vorobtsova et al. 2016). To the best of our knowledge, no other study to date has considered the effect of diameter variations in tortuous coronaries, yet it is clear that tortuosity and diameter would both affect the local haemodynamics (Beier et al. 2016). Therefore, we sought to analyse the haemodynamic changes with respect to vascular diameter in a range of tortuous coronary arteries.

2. Methods

2.1 Vessel Geometries

A total of 28 models were constructed from eight patient-specific coronary geometries — four were left main (LM) bifurcations, and an additional four non-bifurcating arteries, including two Left Anterior Descending (LAD) and two Left Circumflex (LCx).

For each of the LM bifurcation (n = 4), we up- and down-scaled the geometry by 1 mm in centreline diameter corresponding to the original model (Figures 1[c]), forming a collection of 12 bifurcating geometries (4 × 3). Whereas for the non-bifurcating LAD or LCx segments (n = 4), we first modified these to exhibit a constant diameter by sweeping a circular cross section along the centreline with a diameter equivalent to the original mean diameter (Figure 2[a]). These were then both scaled-up and -down by 1 mm in orthogonal direction each (Figure 2[b]), forming a collection of 16 non-bifurcating geometries (4 × 3 plus 4 original varying cross-sectional diameter models). All final diameter variations were within the normal physiological range (Medrano-Gracia et al. 2016).

Since tortuosity is a centreline-based parameter, all modified geometries exhibited the same tortuosities as their original ones, as the shape of centrelines had not been changed. For all models, the inlet was extended 1.5 times the respective inlet diameter to assure a fully developed flow profile generated in the region of interest.

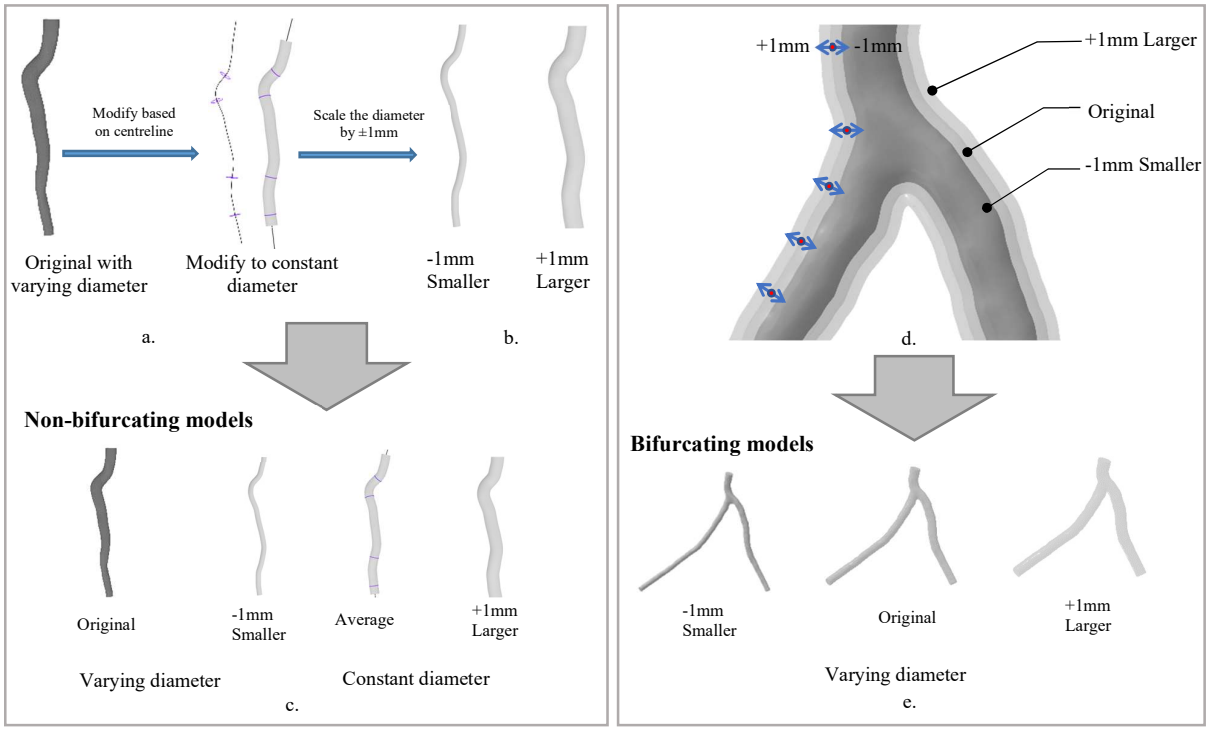

Figure1. Geometry modelling: (a) reconstruction of idealised non-bifurcating arteries. Circular cross-sectional lumen areas were generated based on centreline, which resulted the idealised models by sweeping. (b) Idealised models with smaller and larger constant diameters. (c) Diameter-scaled non-bifurcating models (d) Illustration of inflation and deflation (e) Diameter-scaled bifurcating models.

2.2 Computational Simulations

All models were numerically resolved using the commercially available Navier-Stokes solver ANSYS-CFX (Canonsburg, PA). The flow was assumed to be laminar, with the blood modelled as a Carreau-Yasuda non-Newtonian fluid (Gijsen et al. 2019). A pulsatile flow profile was specified at the inlet, and a reference pressure condition of 0 Pa was adopted at all the outlets (Beier et al. 2016). An allometric scaling law was used to scale the average coronary inflow with the artery diameter (Gijsen et al. 2019):

$$Q = 1.43d^{2.55} \tag{1}$$

where Q is the cycle-averaged flow rate entering the artery and d is the mean diameter of the inflow segment. The vascular wall was assumed to be rigid, and a no-slip condition was applied. The simulations were first run in a steady-state condition, with the result employed to be the initial condition for the subsequent transient simulation of four consecutive cardiac cycles. All haemodynamic parameters were extracted from the fourth cycle to minimise the transient start-up effects.

2.3 Post-Processing

Streamlines and TAWSS of all models were visualised. Helical flow (HF) was examined using iso-surfaces corresponding to the local normalised helicity (LNH), where a positive value (red) indicates the right-handed rotational patterns, and a negative value (blue) indicates the left-handed flow rotation. The helicity intensity (h_2) was calculated as follows:

$$h_2 = \frac{1}{T\,V}\int_0^T \oiint_V |\boldsymbol{v}(\boldsymbol{x},t)\cdot\boldsymbol{\omega}(\boldsymbol{x},t)|dVdt \tag{2}$$

where $\boldsymbol{v}(\boldsymbol{x},t)$ and $\boldsymbol{w}(\boldsymbol{x},t)$ are the respective velocity and vorticity vectors, T is the cardiac cycle, V is the volume of the fluid domain, and $\oiint_V$ represents the volumetric integral over the fluid domain. Low WSS has adverse impact on endothelium functions, which was reported to induce formation and progression of atherosclerosis (Gijsen et al. 2019; Secomb 2016) . Here, we calculated the percentage of the vascular surface (TAWSS%) exposed to adversely low TAWSS (< 0.5 Pa) (Beier et al. 2016; Gijsen et al. 2019) according to:

$$TAWSS\% = \frac{area\ expposed\ to\ adverse\ TAWSS}{total\ surface\ area\ of\ geometry} \tag{3}$$

3. Results

3.1 Non-bifurcating models

The streamlines colour-coded by velocity and TAWSS contours of a representative non-bifurcating coronary with the geometries derived from it are shown in Figure 2. Compared to the original diameter-varying coronary, the model with a constant diameter equivalent to the original

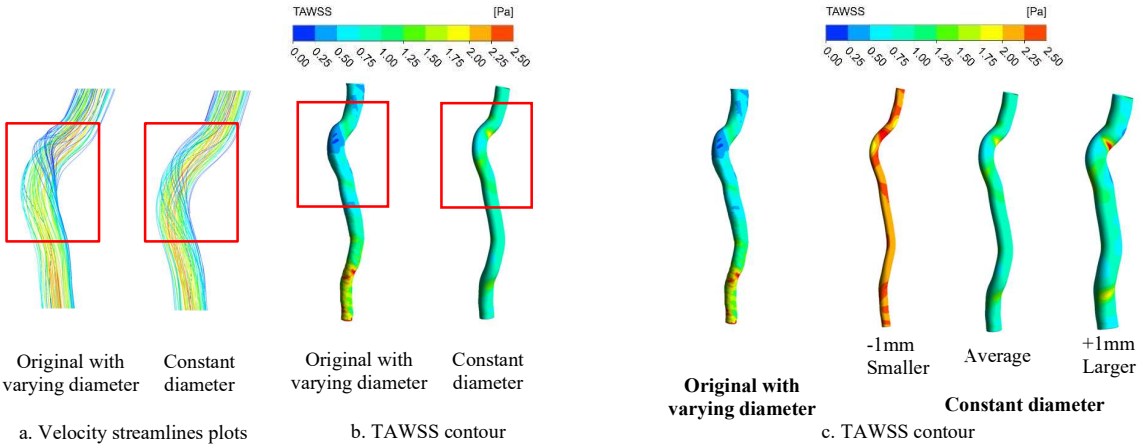

Figure 2. Velocity streamlines plots and TAWSS contours of non-bifurcating models

mean diameter showed less changes within the tortuous segments (indicated as a red rectangle in Figure 2.a), in terms of the velocity. Observed from the TAWSS contours within the tortuous segments (Figure 2.b), the original changing diameter models exhibited a larger TAWSS% (more blue area).

For the constant diameter models (Figure 2.c), the TAWSS% increased with respect to the increase in diameter. However, the original models with varying cross-sectional diameters had the highest TAWSS%, larger than any of the models derived from them, regardless of the size of the diameter (Figure 2. C).

3.2 Bifurcating models

Figure 3.a shows the LNH plots of all bifurcating coronaries with their derived geometries. A pair of counter-rotating HF with apparent asymmetry existed in each model. Smaller models exhibit smaller HF structures (Figure 3.a), which gradually increased with respect to the diameter scale changing from the smaller, to the medium, then to the larger, also evident by the changes in h_2 (Table 1). Compared to the medium models, h_2 was reduced by 24% in the smaller models and increased by 31% in the larger models.

The TAWSS distributions (Figure 3.b) showed the same tendency that the models with a larger diameter had a larger TAWSS% (more blue area). The TAWSS% was reduced by 33% in the smaller diameter models and increased by 44% in the larger model compared to their medium size equivalents.

4. Discussion

This study has investigated the haemodynamic effects of diameter variation in tortuous patient-specific coronary arteries. Overall, results showed that vessel diameter plays an important role alongside the vascular tortuosity, which cannot be assessed independently of each other when their impact on the local haemodynamics is studied. Not only differences in the magnitude of the vascular diameter, but also variations in the diameter along the centreline would lead to drastic alterations of the local haemodynamics, in terms of the HF and TAWSS%.

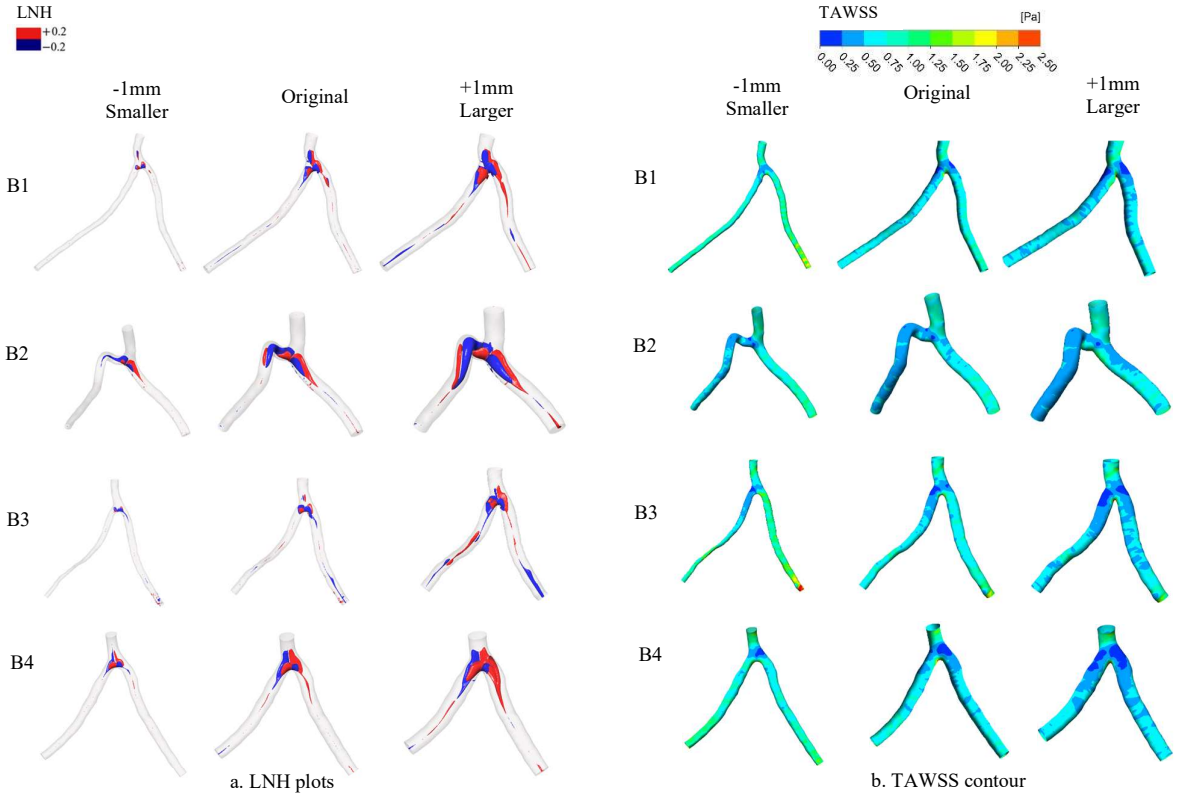

Figure 3. Visualisations of the LNH and TAWSS for bifurcating models

	h_2	TAWSS%	h_2 Difference	TAWSS% difference
B1 original	0.72	15%		
B1 -1 mm smaller	0.56	7%	23%	56%
B1 +1 mm larger	0.93	31%	29%	102%
B2 original	0.65	36%		
B2 -1 mm smaller	0.43	22%	34%	38%
B2 +1 mm larger	0.94	45%	45%	26%
B3 original	0.76	18%		
B3 -1 mm smaller	0.66	14%	13%	13%
B3 +1 mm larger	0.91	33%	21%	21%
B4 original	0.75	21%		
B4 -1 mm smaller	0.55	7%	27%	27%
B4 +1 mm larger	0.98	37%	30%	30%

Table 1. h_2 and TAWSS% of bifurcating models

Models with constant diameters manifested less flow disturbance and a reduced TAWSS% compared to those with varying diameters, although they had exactly the same tortuosities (Figure 2.a). For all models, an increase in diameter was associated with increases in the adverse TAWSS and HF (Figure 2.c, Table 1). Out of relevant literature considering tortuosity, four previous studies (Xie et al. 2014; Buradi and Mahalingam 2020; Xie, Wang, and Zhou 2013; Rabbi, Laboni, and Arafat 2020) have investigated the changes in haemodynamics with respect to tortuosity without considering the diameter effect by assuming constant diameters. In the context of our findings, their conclusions would then need to be reconsidered in terms of vessel diameter.

Some limitations of this work should be noted. First, we tested the diameter only, whereas it is likely that other shape characteristics also play a role in affecting the resulting haemodynamics and should be considered in combination (Beier et al. 2016) Second, further studies are warranted into the role of frequency of the variation in diameter along with other shape characteristics and their possible overall effects on the resulting overall haemodynamics. Moreover, flow conditions may vary in vivo, whereas no patient-specific inflow condition was available, although for illuminating the effect of shape characteristics our computational approach can be considered current best practice.

4. Conclusion

A change in diameter influences the resulting haemodynamics, even for vessels with the same tortuosity, suggesting that studies on patient-specific tortuosity also need to consider the variations in diameter and possibly other vessel shape characteristic. This may explain contradicting findings in previous literature where tortuosity and its haemodynamic effects were assessed independently of other vessel shape characteristics.

Acknowledgments

The authors wish to acknowledge the assistance of resources from KATANA (https://doi.org/10.26190/669x-a286) from UNSW.

References

Beier, Susann, John Ormiston, Mark Webster, John Cater, Stuart Norris, Pau Medrano-Gracia, Alistair Young, and Brett Cowan. 2016. 'Impact of bifurcation angle and other anatomical characteristics on blood flow - A computational study of non-stented and stented coronary arteries', Journal of Biomechanics, 49: 1570-82.

Buradi, Abdulrajak, and Arun Mahalingam. 2020. 'Impact of coronary tortuosity on the artery hemodynamics', Biocybernetics and Biomedical Engineering, 40: 126-47.

El Tahlawi, Mohammad, Amal Sakrana, Abdelrahman Elmurr, Mohammad Gouda, and Marwa Tharwat. 2016. 'The relation between coronary tortuosity and calcium score in patients with chronic stable angina and normal coronaries by CT angiography', Atherosclerosis, 246: 334-37.

Gijsen, Frank, Yuki Katagiri, Peter Barlis, Christos Bourantas, Carlos Collet, Umit Coskun, Joost Daemen, Jouke Dijkstra, Elazer Edelman, Paul Evans, Kim van der Heiden, Rod Hose, Bon-Kwon Koo, Rob Krams, Alison Marsden, Francesco Migliavacca, Yoshinobu Onuma, Andrew Ooi, Eric Poon, Habib Samady, Peter Stone, Kuniaki Takahashi, Dalin Tang, Vikas Thondapu, Erhan Tenekecioglu, Lucas Timmins, Ryo Torii, Jolanda Wentzel, and Patrick Serruys. 2019. 'Expert recommendations on the assessment of wall shear stress in human coronary arteries: existing methodologies, technical considerations, and clinical applications', European Heart Journal, 40: 3421-33.

Kahe, Farima, Sadaf Sharfaei, Anmol Pitliya, Mehrian Jafarizade, Soroush Seifirad, Shaghayegh Habibi, and Gerald Chi. 2020. 'Coronary artery tortuosity: a narrative review', Coronary Artery Disease, 31.

Kashyap, Vishesh, Ramtin Gharleghi, Darson D. Li, Lucy McGrath-Cadell, Robert M. Graham, Chris Ellis, Mark Webster, and Susann Beier. 2022. 'Accuracy of vascular tortuosity measures using computational modelling', Scientific Reports, 12: 865-65.

Khosravani-Rudpishi, Mohsen, Adel Joharimoghadam, and Elham Rayzan. 2018. 'The significant coronary tortuosity and atherosclerotic coronary artery disease; What is the relation?', Journal of cardiovascular and thoracic research, 10: 209-13.

Li, Yang, Yi Feng, Genshan Ma, Chengxing Shen, and Naifeng Liu. 2018. 'Coronary tortuosity is negatively correlated with coronary atherosclerosis', Journal of International Medical Research, 46: 5205-09.

Medrano-Gracia, Pau, John Ormiston, Mark Webster, Susann Beier, Alistair Young, Chris Ellis, Chunliang Wang, Örjan Smedby, and Brett Cowan. 2016. 'A computational atlas of normal coronary artery anatomy', EuroIntervention, 12: 845-54.

Muller, Olivier, Stylianos A. Pyxaras, Catalina Trana, Fabio Mangiacapra, Emanuele Barbato, William Wijns, Charles A. Taylor, and Bernard De Bruyne. 2012. 'Pressure–Diameter Relationship in Human Coronary Arteries', Circulation: Cardiovascular Interventions, 5: 791-96.

Rabbi, Md Foysal, Fahmida S. Laboni, and M. Tarik Arafat. 2020. 'Computational analysis of the coronary artery hemodynamics with different anatomical variations', Informatics in Medicine Unlocked, 19.

Secomb, Timothy W. 2016. 'Hemodynamics.' in, Comprehensive Physiology (Wiley).

Vorobtsova, Natalya, Claudio Chiastra, Mark A. Stremler, David C. Sane, Francesco Migliavacca, and Pavlos Vlachos. 2016. 'Effects of Vessel Tortuosity on Coronary Hemodynamics: An Idealized and Patient-Specific Computational Study', Annals of Biomedical Engineering, 44: 2228-39.

Xie, Xinzhou, Yuanyuan Wang, and Hu Zhou. 2013. 'Impact of coronary tortuosity on the coronary blood flow: A 3D computational study', Journal of Biomechanics, 46: 1833-41.

Xie, Xinzhou, Yuanyuan Wang, Hongmin Zhu, and Jingmin Zhou. 2014. 'Computation of hemodynamics in tortuous left coronary artery: A morphological parametric study', Journal of Biomechanical Engineering, 136.